

Reactive compatibilization of poly(styrene-*ran*-acrylonitrile)/poly(ethylene) blends through the acid-epoxy reaction

Amardeep Gill, Celestine Hong, Daniel Gromadzki,* Milan Marić

Department of Chemical Engineering, McGill University, Montreal, QC H3A 2B2, Canada

*Present address: J. Heyrovský Institute of Physical Chemistry, Academy of Sciences of the Czech Republic,

Dolejšková 3 CZ-18223, Prague 8, Czech Republic

Correspondence to: M. Maric (E-mail: milan.maric@mcgill.ca)

ABSTRACT: Two families of acid functional styrene/acrylonitrile copolymers (SAN) for application as dispersed phase barrier materials in poly(ethylene) (PE) were studied. One type is SAN made by nitroxide mediated polymerization (NMP), which was subsequently chain extended with a styrene/*tert*-butyl acrylate (S/*t*BA) mixture to provide a block copolymer (number average molecular weight $M_n = 36.6 \text{ kg mol}^{-1}$ and dispersity $D = 1.34$, after which the *tert*-butyl protecting groups were converted to acid groups (SAN-*b*-S/AA). The other acid functional SAN is made by conventional radical terpolymerization (SAN-AA). SAN-AA and SAN-*b*-S/AA were each melt blended with PE grafted with epoxy functional glycidyl methacrylate (PE-GMA) at 160 °C in a twin screw extruder (70:30 wt % PE-GMA:SAN co/terpolymer). The non-reactive PE-*g*-GMA/SAN blend had a volume to surface area diameter $\langle D \rangle_{vs} = 3.0 \mu\text{m}$ while the reactive blends (via epoxy/acid coupling) (PE-GMA/SAN-*b*-SAA and PE-GMA/SAN-AA) had $\langle D \rangle_{vs} = 1.7 \mu\text{m}$ and $1.1 \mu\text{m}$, respectively. After thermal annealing, the non-reactive blend coarsened dramatically while the reactive blends showed little signs of coarsening, suggesting that the acid/epoxy coupling was effective for morphological stability. © 2016 Wiley Periodicals, Inc. *J. Appl. Polym. Sci.* **2016**, *133*, 44178.

KEYWORDS: blends; copolymers; radical polymerization; synthesis and processing

Received 8 May 2016; accepted 4 July 2016

DOI: 10.1002/app.44178

INTRODUCTION

Poly(acrylonitrile) (PAN) has been extensively studied for its excellent barrier properties against gases such as oxygen and carbon dioxide.¹ Furthermore, in the food industry, it has been used to block the permeation of aromas and/or flavors in addition to hydrophobic compounds.² Its hydrophilic nature, however, limits its barrier properties/absorption against water vapor² but it could be very effective against hydrocarbon permeation. One key limitation of PAN is its processability; the homopolymer degrades before it melts, making processing very difficult.^{3–6} Therefore, much effort has focused upon copolymerizing AN with different monomers.^{2,6–12} While not all of the studies were done for the purpose of barrier materials, these studies suggest opportunities to use the barrier properties of AN in the form of a copolymer, provided sufficient AN is incorporated. Besides statistical copolymerization, block copolymers containing AN have been made, which provides another route to incorporating PAN's barrier properties.^{13–25} The ability to polymerize AN by radical polymerization techniques, particularly by reversible activation/de-activation polymerization (RADP) techniques such as reversible addition fragmentation transfer (RAFT), atom transfer radical polymerization (ATRP), and nitroxide mediated polymerization

(NMP), makes the subsequent polymer interesting for barrier materials as the microstructure can be tuned in many possible ways due to the possibility of forming block copolymers. Additionally, properties can be further combined into the AN containing (co)polymers by blending with other polymers. To make barrier materials based on a poly(ethylene) (PE) matrix (such as that used for hydrocarbon storage), for example, it is vital to blend the AN-containing copolymer so that the domains can be easily controlled and stable upon further annealing. However, many cases have demonstrated the instability and/or large domains of the dispersed phase when blending either homopolymers, copolymers, or a mixture of both.^{26–33} While much research has been done on adding pre-made compatibilizers,^{6,27–29,31,33–40} most industrial blends are reactively compatibilized and we have focused on using this latter method, like many others.^{30,32,37,41–47} Our focus has been to synthesize AN-rich copolymers with controlled microstructure by NMP which can be further tuned/manipulated by reactive blending. We have focused on amine functional styrene/acrylonitrile (SAN) copolymers blended with poly(ethylene) grafted with maleic anhydride, which revealed a significant decrease in dispersed phase size and a stable morphology.³² In this work, we investigate SAN copolymers with

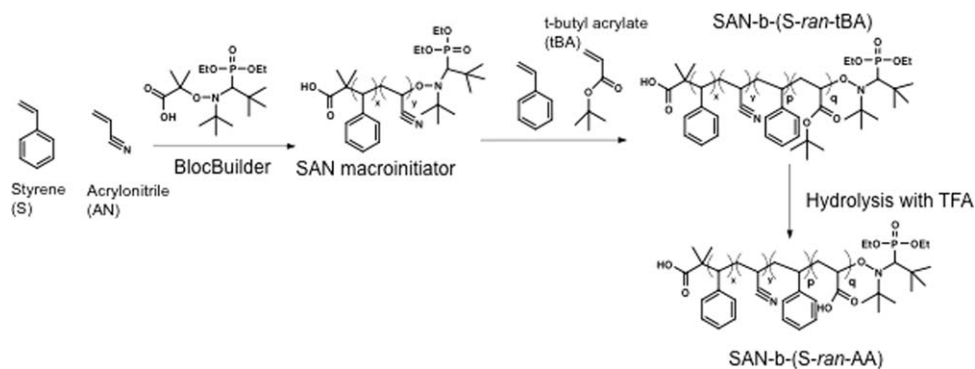


Figure 1. Route to make acrylic acid functional styrene/acrylonitrile (SAN) copolymers. First, the SAN macroinitiator is formed by copolymerization with BlocBuilder unimolecular initiator. Then, the SAN macroinitiator starts the copolymerization of styrene with *t*-butyl acrylate (*t*BA) to make a SAN-*b*-P(*S*-*ran*-*t*BA) block copolymer. Finally, the *t*-butyl protecting groups are cleaved, to leave the pendant acid functional SAN-*b*-(*S*-*ran*-AA) copolymer.

an acid functionality (via incorporation of acrylic acid (AA)) to use with PE grafted with epoxy-functional glycidyl methacrylate (PE-*g*-GMA). The carboxylic acid/epoxy coupling reaction is convenient, due to the ease in which an acid functionality can be inserted directly or indirectly through chemical modification and commercial availability of PE-*g*-GMA. The acid/epoxy reaction has been shown to have a relatively low conversion (10% in 2 min at 180 °C) compared to the primary amine/maleic anhydride coupling, but a much higher conversion compared to other couplings such as amine/acid, acid/hydroxyl, acid/oxazoline, and, amine/epoxy.^{48,49} The acid/epoxy coupling has not been uniformly effective in some blend systems, particularly in highly incompatible blends with relatively thin interfaces.³⁰ SAN blends have been more focused on using the amine/maleic anhydride reaction, even though the synthesis of a relatively cheap amine-functional monomer is required.^{30,49–53} Therefore, using monomers that are commercially available is attractive and an acid functional terpolymer S/AN/AA was thus targeted here. Initially, conventional radical polymerization was used to determine the sensitivity of copolymer composition to initial monomer composition. Afterwards, a controlled radical polymerization technique, NMP, was used to make the acid-functional SAN copolymers and by means of chain extension from a macroinitiator, the acid groups will be incorporated as side groups on one end of the chain. In contrast to earlier work and the previous study,³² where a single functionality was located terminally as a single unit, this study attempts to place several acid groups along the SAN copolymer chains (Figure 1). Functional groups located terminally are more reactive than ones placed randomly in the polymer⁵⁴ but the higher concentration of functional groups is expected to increase the probability of reaction with the complementary functional group. This would lead to more graft copolymer being formed *in situ* and better stabilization of the dispersed SAN phase in the PE matrix and thus lead to potential new barrier materials for PE based on SAN inclusions.

EXPERIMENTAL

Materials

Styrene (99%), *tert*-butyl acrylate (99%, *t*-BA), and AN (99%) were obtained from Sigma–Aldrich (Oakville ON Canada) and purified by passing them through a column of aluminum oxide (Brockmann, Type 1, 150 mesh, Sigma–Aldrich) and calcium hydride

(90–95% reagent grade, Sigma–Aldrich) which were mixed at a mass ratio of 5:0.25, respectively, and stored under a head of nitrogen prior to use. AIBN was obtained from Dupont (Wilmington DE), dissolved in methanol, and re-crystallized before use. Acrylic acid (AA, 99%), trifluoroacetic acid (99%), deuterated chloroform (CDCl₃, 99.8 atom %), and deuterated dimethylsulfoxide (DMSO-*d*₆, 99.96 atom %) were obtained from Sigma–Aldrich and were used as received. BlocBuilder (BB) was provided by Arkema (King of Prussia, PA) and was transformed to a succinimidyl ester functionalized form of BB known as NHS-BlocBuilder (NHS-BB) using an established protocol.⁵⁵ 1,4-Dioxane (99%) and *n*-hexanes (98.5%) were obtained from Fisher (Ottawa, ON Canada) and were used as received. Finally, HPLC grade tetrahydrofuran (THF, 99.9%) was obtained from Fisher as the mobile phase for GPC and was used as received. PE grafted with glycidyl methacrylate (PE-*g*-GMA) (8.46 wt %) with a melt flow index of 4.88 g (10 min)^{−1} at 190 °C, density of 0.94 g mL^{−1}, melting point of 106 °C was obtained from Arkema (Exton, PA) and used as received. Acetone (99.5%) and methanol (99.8%) were obtained from Fisher and used as received.

Methods

Synthesis of Styrene/Acrylonitrile Copolymers. Styrene (S) and AN were copolymerized via conventional radical polymerization using 1,4-dioxane as the solvent in a three necked 50-mL round bottom flask reactor with a nitrogen purge, thermocouple/thermowell, and reflux condenser. The reactor sat on top of a stirring plate and heating mantle. Appropriate amounts of the AIBN initiator, S, AN, and 1-4 dioxane were weighed and poured into the reactor, with the formulation for S_AN_Exp1 (see Table I) shown as an example. For this particular experiment, 0.1217 g (0.740 mmol) AIBN, 4.8471 g (46.54 mmol) S, 1.50 g (28.27 mmol) AN, and 6.7582 g (76.70 mmol) 1,4-dioxane were measured and poured into the reactor. The reactor solution was purged with nitrogen for at least 30 min prior to starting the reaction and maintained throughout the reaction. The set point of the reactor was set to 70 °C to ensure significant decomposition of the initiator.⁵⁶ The chiller was set to 4 °C. Once the reaction was complete (reaction time of 3–4 h), the polymer was precipitated first in about 200 mL of hexane, re-dissolved in a minimum amount of solvent, and precipitated a second time in about 50 mL of hexane to further remove unreacted monomers. Finally, the polymer was vacuum dried in an oven at 50–60 °C overnight. This particular copolymer had

Table I. Characterization of Non-Reactive SAN Copolymers Synthesized by Conventional Radical Polymerization

Experiment ID	Feed composition			Characterization			
	[AIBN] (mM)	[S] (M) ^a	[AN] (M) ^a	$f_{S,0}$ ^b	F_S ^c	M_n (kg mol ⁻¹) ^d	\bar{D} ^d
S_AN_Exp1	54.0	3.39	2.06	0.62	0.62	62.7	1.76
S_AN_Exp2	44.8	3.93	1.40	0.74	0.76	34.5	1.80
S_AN_Exp3	33.2	4.03	0.59	0.87	0.85	35.2	1.72
S_AN_Exp4	36.4	2.08	4.58	0.31	0.52	N/A ^e	N/A ^e

^a 50:50 wt % monomers to solvent ratio.

^b Initial composition of styrene in the monomer mixture.

^c Styrene mol fraction in the copolymer (calculated using ¹H-NMR).

^d Obtained by GPC using THF as the mobile phase with respect to PMMA standards at 40 °C.

^e The final copolymer molecular weight was not measured by GPC since it was insoluble in the THF solvent.

$M_n = 62.7 \text{ kg mol}^{-1}$ and $\bar{D} = 1.76$ relative to PMMA standards at 40 °C in THF. The copolymer had an S molar composition of 0.63, which was determined by ¹H-NMR (300 MHz, CDCl₃, δ): 6.9–7.5 (m, 5H, Ar H), 1.2–2 (m, 2H, CH₂). The copolymers were also analyzed qualitatively by FTIR: 2250 (s; $\nu(\text{C}\equiv\text{N})$).

Synthesis of Styrene/Acrylonitrile/Acrylic Acid Terpolymers by Conventional Radical Polymerization. S, AN, and AA were polymerized via conventional radical polymerization using 1,4-dioxane as the solvent in a three necked 50-mL reactor with a nitrogen purge, thermocouple/thermowell, and reflux condenser. The reactor sat on top of a stirring plate and heating mantle. Appropriate amounts of AIBN, S, AN, AA, and, 1,4-dioxane, were weighed and poured into the reactor, with the formulation for S_AN_AA_1 (see Table II) shown as an example. For this particular experiment, 0.10537 g (0.64 mmol) AIBN, 5.4704 g (52.52 mmol) S, 2.0955 g (39.49 mmol) AN, 1.945 g (26.99 mmol) AA, and, 10.0471 g (114.03 mmol) 1,4-dioxane were poured into the reactor. The reactor solution was purged with nitrogen for at least 30 min prior to starting the reaction. The set point of the reaction was set to 70 °C. The chiller was set to 4 °C.

Table II. formulations for the Synthesis of Styrene/Acrylonitrile/Acrylic Acid (S/AN/AA) Terpolymers by Conventional Radical Polymerization

Expt. ID ^a	[AIBN] (mM)	[S] ₀ (M) ^b	[AN] ₀ (M) ^b	[AA] ₀ (M) ^b	$f_{S,0}$	$f_{AA,0}$
S_AN_AA_1	31.8	2.60	1.96	1.34	0.44	0.23
S_AN_AA_2	30.3	3.41	0.90	1.16	0.62	0.21
S_AN_AA_3	32.2	2.68	2.20	1.20	0.44	0.20
S_AN_AA_4	32.3	3.51	0.84	1.09	0.65	0.20
S_AN_AA_5	34.2	3.82	0.30	1.03	0.74	0.20
S_AN_AA_6	32.3	3.45	0.77	1.23	0.41	0.25
S_AN_AA_7	33.3	3.49	0.83	1.08	0.65	0.20
S_AN_AA_8	32.7	3.81	0.39	0.91	0.75	0.18
S_AN_AA_9	36.0	2.61	0.92	2.36	0.44	0.40
S_AN_AA_10	37.8	3.10	0.93	1.66	0.55	0.30
S_AN_AA_1	31.8	2.60	1.96	1.34	0.44	0.23

^a 50:50 wt % monomers to solvent ratio.

^b The initial molar concentrations of styrene, acrylonitrile, and acrylic acid in the mixture are given by [S]₀, [AN]₀, and [AA]₀, respectively.

After heating at 70 °C for 2–3 h, the polymer was precipitated first in about 200 mL of hexane, re-dissolved in a minimum amount of solvent, and precipitated a second time in about 50 mL of hexane to remove unreacted monomers. Finally, the polymer was vacuum dried in the oven at 50–60 °C overnight. This particular copolymer had $M_n = 42.5 \text{ kg mol}^{-1}$ and $\bar{D} = 1.65$ relative to PMMA standards at 40 °C in THF. The terpolymer had S and AN molar composition of 0.26 and 0.67 respectively, which was determined by ¹H-NMR (300 MHz, CDCl₃, δ): 6.9–7.5 (m, 5H, Ar H), 0.8–2 (m, 3H, CH—CH₂), 3.7 (s, 3H, O=CH₃). The copolymers were also analyzed qualitatively by FTIR: 1650–1750 (s; $\nu(\text{C}=\text{O})$), 2250 (s; $\nu(\text{C}\equiv\text{N})$), 3000 (s; $\nu(\text{COOH})$).

Synthesis of SAN Copolymers by Nitroxide Mediated Polymerization. S and AN were copolymerized via NMP using 1,4-dioxane as the solvent in a three necked 50-mL reactor with a nitrogen purge, thermocouple/thermowell, and reflux condenser. The reactor sat on top of a stirring plate and heating mantle. Appropriate amounts of NHS-BB, S, AN, and 1,4-dioxane were measured out and poured into the reactor, with the formulation for S_AN_NHS-BB-1 (see Table V) shown as an example. For this particular experiment, 0.1805 g (0.38 mmol) NHS-BB, 9.4527 g (90.76 mmol) S, 0.5698 g (10.74 mmol) AN, and 10.1038 g (114.67 mmol) 1,4-dioxane were measured and poured into the reactor. The reactor solution was purged with nitrogen for at least 30 min prior to starting the reaction and maintained throughout the reaction. The set point of the reaction was set to 115 °C. The chiller was set to 4 °C. Once the reaction was complete after 4–5 h, the polymer was precipitated the first time in about 200 mL of hexane, re-dissolved in a minimum amount of solvent, and precipitated a second time in about 50 mL of hexane to remove unreacted monomers. Finally, the polymer was vacuum dried in the oven at 50–60 °C overnight. This particular copolymer had M_n of 7.0 kg mol⁻¹ and \bar{D} of 1.18 by GPC relative to PMMA standards at 40 °C in THF. The copolymer had S composition of 0.93 and a conversion of 0.38, which were both determined by ¹H NMR (300 MHz, CDCl₃, δ): 6.9–7.5 (m, 5H, Ar H), 1.2–2 (m, 2H, CH₂). The copolymers were also analyzed qualitatively by FTIR: 2250 (s; $\nu(\text{C}\equiv\text{N})$).

Chain Extension of Styrene/Acrylonitrile Copolymer Macroinitiators with Styrene/*Tert*-Butyl Acrylate by Nitroxide Mediated Polymerization. Chain extension was done on the final SAN copolymer synthesized (with a S molar composition

of 0.62, see Table VI) in 1,4-dioxane with the same setup described for the other NMP experiments. A *S/t*-BA mixture at a mole ratio of 50/50 was mixed in with the SAN copolymer and 1,4-dioxane. The macro-initiator (SAN) was rich in AN to give the first block significant barrier properties (typical barrier materials have 40–50 mol % AN).⁵⁵ The chain extension was done at 100 °C. After approximately 1.5 h, the polymerization was stopped by cooling the mixture. Once the product was purified by air drying (due to difficulty in precipitation) and vacuum dried at 60 °C, the *t*-BA groups were converted to acid groups (SAN-*b*-SAA) using a published protocol with trifluoroacetic acid.⁵⁷ The SAN copolymer had a M_n of 10 kg mol⁻¹ and \bar{D} of 1.23, and the block copolymer had a M_n of 36.6 kg mol⁻¹ and \bar{D} of 1.34 relative to PMMA standards at 40 °C in THF. The block copolymer was also analyzed qualitatively by FTIR post-acidification: 1650–1750 cm⁻¹ (s; ν (C=O)), 2250 cm⁻¹ (s; ν (C≡N)), 3000 cm⁻¹ (s; ν (COOH)).

Characterization

Proton Nuclear Magnetic Resonance. The composition of all polymers was determined by ¹H-NMR (Varian 300 MHz). The peaks of interest for SAN copolymers were at $\sim\delta = 6.5$ –7 ppm for the five styrenic protons and $\delta = 1.2$ –2 ppm for the backbone protons. The peaks of interest for the *S/AN/AA* terpolymers and SAN-*b*-SAA were at $\delta = 6.5$ –7 ppm for the five styrenic protons, $\delta = 0.8$ –2 ppm for the backbone protons, and $\delta = 3.6$ ppm for methyl protons of AA which had been previously methylated with a trimethylsilyldiazomethane solution.⁵⁷ For all polymers, the AN content was calculated using the backbone CH₂ protons rather than solely the proton on the α -carbon.^{7,12}

For kinetic studies, conversion was calculated using ¹H-NMR. Specifically, the vinyl protons were used for each monomer, none of which overlapped. DMSO-*d*₆ was used as the solvent for ¹H-NMR to calculate conversion for the kinetic studies. It was used instead of CDCl₃ to avoid interference with the signal due to S. CDCl₃ was used to determine polymer compositions.

Gel Permeation Chromatography. All polymers were analyzed using a Waters Breeze system equipped with three Styragel columns (molecular weight ranges: HR1: 10²–5 × 10³ g mol⁻¹, HR2: 5 × 10²–2 × 10⁴ g mol⁻¹, HR3: 5 × 10³–6 × 10⁵ g mol⁻¹) and a guard column. The flow rate was 0.3 mL min⁻¹. The Gel Permeation Chromatography (GPC) was equipped with a differential refractive index (RI 2410) detector. All polymers were analyzed with THF as the mobile phase at a column temperature of 40 °C. The molecular weights were measured relative to PMMA standards. Prior to analysis, polymer samples containing AA were methylated with a trimethylsilyldiazomethane solution (2 M in hexanes) to prevent sticking of the acid groups onto the column.⁵⁷

Attenuated Total Reflection-Fourier Transform Infrared Spectroscopy. A Perkin-Elmer spectrum TWO with UATR accessory (also from Perkin-Elmer) and diamond as the attenuated total reflection (ATR) crystal was used to qualitatively analyze SAN copolymers, *S/AN/AA* terpolymers, and the chain extension. The peak of interest for SAN copolymers was $\nu = 2200$ cm⁻¹ for the nitrile stretch for AN.⁵⁸ The peaks of interest for *S/AN/AA* terpolymers and SAN-*b*-SAA were at $\nu = 1600$ –1800 cm⁻¹ for the

carbonyl stretch of AA, $\nu = 2200$ cm⁻¹ for the nitrile stretch for AN, and $\nu = 3000$ cm⁻¹ for the O—H stretch of the acid to ensure that the carbonyl peak did not represent unconverted/unreacted *t*-BA (further evidence of this was obtained from the ¹H-NMR spectrum).⁵⁸

Thermal Gravimetric Analysis. A thermal gravimetric analysis (TGA) Q500 from TA Instruments was used to determine the minimum degradation temperature and degradation profiles of the *S/AN/AA* terpolymers. The analysis was done from nearly ambient temperature (35–40 °C) to 550 °C at a heating rate of 10 °C min⁻¹. The analysis was done under oxygen rather than nitrogen to simulate the environment in an extruder.

Differential Scanning Calorimetry. A differential scanning calorimetry (DSC) Q2000 from TA Instruments was used to approximate the T_g of the *S/AN/AA* terpolymers. The analysis for *S/AN/AA* terpolymers was comprised of two heating cycles and one cooling cycle. Heating began at -20 °C and went to 160 °C at a rate of 20 °C min⁻¹. The cooling cycle began at 160 °C and went to -20 °C at a rate of 20 °C min⁻¹. The measurements were done in an aluminum *t-zero* pan and were calibrated with an empty aluminum *t-zero* pan.

Extrusion and Scanning Electron Microscopy. SAN copolymers, the terpolymer *S/AN/AA*_8, and the block copolymer SAN-*b*-SAA were each melt blended with PE-*g*-GMA in a Haake MiniLab II twin screw extruder in counter-rotating mode. A 70:30 mass ratio of PE-*g*-GMA:polymer was used. The mixture was manually mixed with a spatula prior to feeding it to the extruder. The operating conditions for the extruder were 160 °C at 50 rpm. The material was passed through the extruder a total of three times before the product was collected (a total residence time of 2–3 min). The product was quenched in liquid nitrogen within the first 10–20 s as it exited on the third pass to preserve the morphology. A sample of the product was freeze-fractured and was put into a beaker of THF (and stirred) for a minimum of 24 h to ensure the dispersed phase was etched out. The samples were dried and glued onto aluminum stubs with cyanoacrylate glue. They were then coated with a 2 nm layer of platinum to make the sample conductive for scanning electron microscopy (SEM) analysis. A FEI Inspect F-50 FE SEM was used to analyze the surfaces of the extruded polymers at 1–2 kV (significant charging occurred at higher settings). Finally, ImageJ was used to analyze the dispersed phase size. A minimum of 350 particles was used in determining the average volume to surface area diameter $\langle D \rangle_{vs}$. The particles were manually selected using the ROI manager rather than letting the software automatically detect particles. The background was subtracted before adjusting the threshold. $\langle D \rangle_{vs}$ of each blend before and after annealing was calculated using eq. (1).⁵³

$$\langle D \rangle_{vs} = \frac{\sum_{i=1}^k n_i D_i^3}{\sum_{i=1}^k n_i D_i^2} \quad (1)$$

Note that n_i is the number of particles and D_i is the diameter of the assumed spherical particle. $\langle D \rangle_{vs}$ was calculated by assuming that the particles were spherical (in 3D) and circular (in 2D) so that their diameter could be extracted from their area.

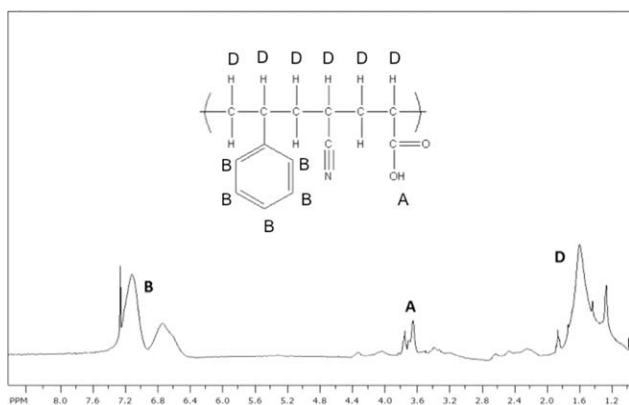


Figure 2. $^1\text{H-NMR}$ spectrum of styrene/acrylonitrile/acrylic acid (S/AN/AA) terpolymer (Sample S_AN_AA_9 from Tables II and III).

Rheology. Sample disks (~ 0.7 g) of PE-g-GMA, SAN copolymer, and SAN-*b*-SAA were prepared in a Carver Model 3857 hot press at 200°C . The disks were 1 mm in thickness and 25 mm in diameter. The discs were prepared between poly(tetrafluoroethylene) plates at a clamping force of 12 tons. The pressing time was 30 min for PE-g-GMA with quick releases at 10 min intervals to remove any air bubbles. The pressing time for the remaining samples was 10 min with quick releases at 3-min intervals. The disks were cooled to room temperature at a rate of about $35^\circ\text{C min}^{-1}$. Rheology measurements were performed on the prepared disks using an Anton Parr MCR 302 parallel plate rheometer using a frequency sweep at 160°C under nitrogen. The strain was kept below 10% to stay within the linear viscoelastic regime and the angular frequency was varied between 0.01 and 300 s^{-1} .

RESULTS AND DISCUSSION

Synthesis of Styrene/Acrylonitrile Copolymers

S was copolymerized with AN using conventional radical polymerization with AIBN as the initiator. These SAN copolymers would serve as non-reactive dispersed phase for subsequent blending with PE. The objective was to make copolymers with a sufficiently high AN content for barrier applications so feed compositions were varied to confirm its incorporation into the copolymers. The data is presented in Table I (Sample S_AN_Exp1).

The compositions were calculated by examining the peak areas for the styrenic protons of S at $\delta = 6.4\text{--}7.2$ ppm (area given as "B"), and the backbone protons of the polymer $\delta = 1.2\text{--}2.0$ ppm (area given by "A") using the following previously published method¹²: $n = \text{moles of S present in copolymer} = \frac{B}{5}$; $m = \text{moles of AN present in copolymer} = \frac{A}{2} - n$.

F_S and F_{AN} were calculated using:

$$F_S = \frac{n}{n+m}; F_{AN} = 1 - F_S$$

Table I shows that the azeotropic composition (i.e., when initial monomer feed composition is equal to copolymer composition) for this system was approximately $f_s = 0.62$, which is very similar to previous studies.^{59–61} Table I also shows that varying the feed composition still results in significant AN incorporation,

which is in agreement with earlier studies.^{11,61} With the confirmation that AN can be incorporated over a wide compositional range, the incorporation of a reactive functionality (carboxylic acid) was attempted via terpolymerization of S, AN, and AA.

Synthesis of Styrene/Acrylonitrile/Acrylic Acid Terpolymers

Initially, methacrylic acid was used with S and AN, but its incorporation was extremely low ($<1\%$ mol). It was hypothesized that the methyl group on the vinyl decreased its reactivity due to steric hindrance.⁶² AA was instead used to incorporate acidic functionality into the SAN copolymer. AA was incorporated into a terpolymer previously by conventional radical polymerization with S and AN.⁶³ Tables II and III show the different feed compositions that were tested to assess how to obtain an adequate AN content ($\sim 40\text{--}50$ mol %) while at the same time to obtain a sufficient AA content to aid in reactive compatibilization (~ 5 mol %). Figure 2 shows a typical $^1\text{H-NMR}$ spectrum of these terpolymers.

The terpolymer compositions were determined by examining the peak for the styrenic protons ($\delta = 6.4\text{--}7.2$ ppm labeled as B), along with the peak for the methyl protons of AA (after methylation) ($\delta = 3.6\text{--}3.8$ ppm labeled as A), and the backbone protons ($\delta = 1.2\text{--}2.0$ ppm labeled as D). The approach is outlined below to determine the mole fractions of the monomers in the terpolymer:

$$X = \text{moles of S in terpolymer} = \frac{B}{5};$$

$$Y = \text{moles of AA in terpolymer} = \frac{A}{3};$$

$$Z = \text{moles of AN in terpolymer} = \frac{D}{3} - X - Y.$$

The initial experiments (S_AN_AA_1 and 3) resulted in an acid incorporation in the desired range of 5–10 mol %. As can be seen from Table III, while the acid content was desirable, the corresponding AN content was >60 mol %, which was sufficiently high to be effective as an oxygen and CO_2 barrier material but hopefully not excessively high that processing would be affected.⁶⁴ Therefore, a wider study of the ternary system was conducted to determine a guideline to obtain sufficient AN and AA compositions. It seems from the small sample set that rather than decreasing the AN initial concentration and increasing the S initial concentration, decreasing the AN initial concentration and increasing the AA initial concentration achieved a more acceptable AN terpolymer composition. Increasing the AA feed content, as can be seen by S_AN_AA_9, can result in high acid terpolymer compositions. However, S_AN_AA_4, 5, and 7 were satisfactory in controlling both the AA composition and achieving sufficient AN content in the terpolymer (4–8 mol % AA and 52–57 mol % AN, respectively). Thermal properties of the terpolymers were characterized via TGA and DSC. From DSC, an inflection point indicated that T_g is slightly above 100°C . The T_g s of all terpolymers are listed in Table IV.

The T_g s of PAN, poly(styrene) and poly(acrylic acid) homopolymers are $90\text{--}100^\circ\text{C}$, as can be suggested by the terpolymers listed in Table IV. There is some variation in T_g as it is not only a function of molecular weight and composition, but of monomer sequencing due to possible interactions and/or steric hindrance between adjacent monomer units.^{65–67} This, along with

Table III. Characterization of Styrene/Acrylonitrile/Acrylic Acid (S/AN/AA) Terpolymers Synthesized by Conventional Radical Polymerization

Experiment ID	Feed composition		Terpolymer composition			Molecular weight distribution	
	$f_{S,0}$	$f_{AA,0}$	F_S^a	F_{AA}^a	F_{AN}^a	M_n (kg mol ⁻¹) ^b	\bar{D}^b
S_AN_AA_1	0.44	0.23	0.26	0.07	0.67	42.5	1.65
S_AN_AA_2	0.62	0.21	0.44	0.04	0.52	34.7	1.43
S_AN_AA_3	0.44	0.20	0.21	0.04	0.75	52.0	1.58
S_AN_AA_4	0.65	0.20	0.44	0.04	0.52	63.0	1.92
S_AN_AA_5	0.74	0.20	0.43	0.04	0.53	55.4	1.71
S_AN_AA_6	0.41	0.25	0.24	0.08	0.68	70.0	1.92
S_AN_AA_7	0.65	0.20	0.35	0.08	0.57	15.6	1.56
S_AN_AA_8 ^c	0.75	0.18	0.67	0.25	0.08	60.1	1.84
S_AN_AA_9 ^c	0.44	0.40	0.67	0.26	0.07	19.4	1.37
S_AN_AA_10	0.55	0.30	0.75	0.04	0.21	74.6	1.81

^aCopolymer composition calculated using ¹H-NMR.

^bObtained by GPC using THF as the mobile with respect to linear PMMA standards at 40 °C.

^cS_AN_AA_8 and S_AN_AA_9 had similar compositions but S_AN_AA_9 was run to a lower conversion (it thus has a lower molecular weight compared to S_AN_AA_8).

the different chain lengths from each sample, explain the variation in T_g of the synthesized terpolymers. DSC provided relevant information regarding the T_g (and therefore, extrusion temperature), but TGA was also performed to understand the degradation process of the terpolymers with Figure 3 as a typical example.

The expected degradation profile of S_AN_AA terpolymers matches Figure 3. Moisture and residual solvent evaporated at about 100 °C. Afterwards, AA began to transform presumably to anhydrides (up to 150 °C) and then to smaller volatilized organic compounds beyond 150 °C.⁶⁸ S and AN decomposed after 250 °C.⁶⁹ It was important to see the early degradation of AA, as this puts a constraint on the temperatures that the terpolymers could be extruded.

Synthesis of Styrene/Acrylonitrile Copolymers by NMP

After confirming that AN could be incorporated into a copolymer with S and into a terpolymer with S and AA, controlled radical polymerization, specifically NMP, was used to synthesize SAN copolymers with chain-end fidelity (possibility of chain extension) to incorporate barrier properties in one block and/or

functional groups in the other. Also, placing functional groups near one end of the chain should improve their accessibility to react with complementary functional groups from the other polymer during blending.⁵⁴ Table V shows the reaction formulations and the characterization of the copolymers that were synthesized—various initial compositions were tested to confirm incorporation of AN in the copolymer macroinitiator.

It can be immediately noticed from Table V that the \bar{D} of the copolymers synthesized is significantly lower than the ones synthesized by conventional radical polymerization, as expected. Furthermore, the copolymer compositions matched well to those previously reported⁷⁰ and our earlier results by conventional radical polymerization. Kinetic studies were also performed for each polymerization to see how well the polymerization mimicked the expected behavior for a controlled mechanism (i.e., linear M_n versus conversion). Typical kinetic plots for one of the polymerizations are shown in Figure 4.

It can be seen from Figure 4 that over the course of the 5-h reaction period, the kinetic plot is relatively linear and show a

Table IV. Glass transition Temperatures of the Terpolymers

Experiment I.D.	F_S	F_{AA}	T_g (°C)	M_n (kg mol ⁻¹)
S_AN_AA_1	0.26	0.07	113.9	42.5
S_AN_AA_2	0.44	0.04	—	34.7
S_AN_AA_3	0.21	0.04	—	52.0
S_AN_AA_4	0.44	0.04	100.3	63.0
S_AN_AA_5	0.43	0.04	82.2	55.4
S_AN_AA_6	0.49	0.18	—	70.0
S_AN_AA_7	0.35	0.08	76.5	15.6
S_AN_AA_8	0.67	0.25	87.5	60.1
S_AN_AA_9	0.67	0.26	105.1	19.4
S_AN_AA_10	0.75	0.04	98.6	74.6

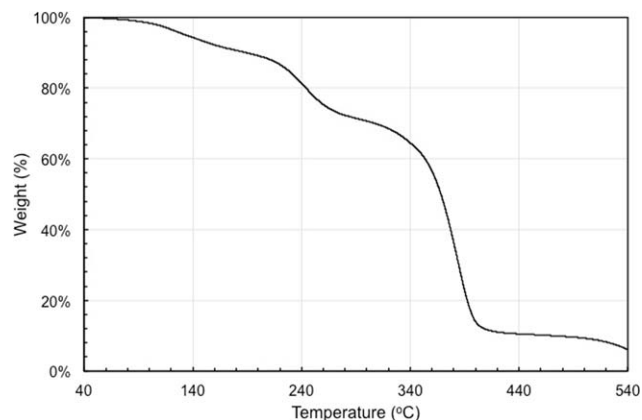
**Figure 3.** TGA analysis of styrene/acrylonitrile/acrylic acid (S/AN/AA) terpolymer (Sample S_AN_AA_1 from Table III).

Table V. Characterization of SAN Copolymers Synthesized by NMP

Experiment ID	Feed composition			Characterization			
	NHS-BB (M)	[S] ₀ (M) ^a	[AN] (M) ^a	<i>f</i> _{S,0}	<i>F</i> _S ^b	<i>M</i> _n (kg mol ⁻¹) ^c	<i>D</i> ^c
S_AN_NHS-BB-1	0.018	4.34	0.51	0.89	0.93	10.0	1.18
S_AN_NHS-BB-2	0.018	4.04	1.09	0.79	0.86	13.5	1.20
S_AN_NHS-BB-3	0.018	3.77	1.60	0.70	0.72	10.6	1.17
S_AN_NHS-BB-4	0.018	3.38	2.22	0.60	0.64	20.0	1.25

^a 50:50 wt % monomers to solvent ratio.^b Calculated using ¹H-NMR.^c Obtained by GPC using THF as the mobile phase with respect to PMMA standards at 40 °C.

steady consumption of monomers over time, with no indication of a plateau that would imply dead chains.^{10,57,71,72} Furthermore, *M*_n versus conversion plots show that the chains are growing linearly over time, which is also an indicator that the polymerization was reasonably controlled with no overt chain termination or transfer suggested.^{10,57,71,72} Otherwise, the kinetic plots demonstrate a linear trend and give an apparent rate constant (the slope of the $\ln\left(\frac{1}{1-x}\right)$ versus time plot) which can be used to estimate $k_p K = 3.2\text{--}5.8 \times 10^{-5} \text{ s}^{-1}$ where k_p is the propagation rate constant and K is the equilibrium constant. k_p for AN is reported to be $1.5 \times 10^4 \text{ L mol}^{-1}$ while for S, k_p is

reported as $1.8 \times 10^3 \text{ L mol}^{-1}$ at the temperature of interest.¹⁸ K for S and AN is $2.2 \times 10^{-9} \text{ mol L}^{-1}$ and $1 \times 10^{-10} \text{ mol L}^{-1}$ respectively at the temperature of interest.⁷⁰ It is not surprising that even though the feed composition was varied, the apparent rate constant did not vary much since the $k_p K$ reported for both S and AN are approximately equal.⁷⁰ Acid functionality was next incorporated to provide the necessary groups for reactive blending.

Synthesis of Block Copolymers Using SAN Copolymers

The ideal goal was to synthesize S/AN/AA terpolymers by NMP so that the acid groups could be randomly distributed in the terpolymer like with conventional radical polymerization, but the terpolymerization yielded little to no acid (<0.5% AA). Using NMP would have provided more chain-to-chain compositional homogeneity and thus could be more effective in compatibilization. Based on the reactivity ratios published in the literature for this ternary system ($r_{AA/S} = 0.12$, $r_{S/AA} = 0.63$, $r_{AN/AA} = 0.68$, $r_{AA/AN} = 0.61$, $r_{AN/S} = 0.09$, $r_{S/AN} = 0.34$), AA should have been incorporated readily into the polymer.⁵⁷ There is some indication that MEHQ inhibitor plays a role in retarding the polymerization of AA.⁷³ It was not removed prior to use, however, the same unpurified AA was successfully used previously with NMP.⁵⁷ Consequently, we chose to use the block copolymer so that the SAN segment is ensured and then the second block consisted of the AA needed for the reactive blending. The formulation and its characterization are listed in Table VI. The first block was a SAN block at the azeotropic feed composition $\sim f_s = 0.60$. The second block was a S/*t*-BA block at an initial monomer composition $f_{S,0} = 0.50$. Due to AA's tendency to attack the SG1 groups of the initiator, the acid functionality was incorporated in the form of a protected version of AA, *t*-BA. The *tert*-butyl groups later can be easily removed by acid hydrolysis, resulting in carboxylic acid functionality.

During the kinetic studies, evidence pointed toward a controlled radical mechanism and the ability to chain extend is confirmation of the chain-end fidelity.^{10,57,71,72} The increase in *M*_n with a monomodal shift in the molecular weight distribution is a good indicator of a successful chain growth, as can be seen from the GPC chromatogram in Figure 5.

A clear shift to the left in the GPC chromatograph, indicative of higher molecular weight chains, indicates that chain extension proceeded. There was not excessive skewness, indicative of a low molecular tail, implying that there was not a significant fraction

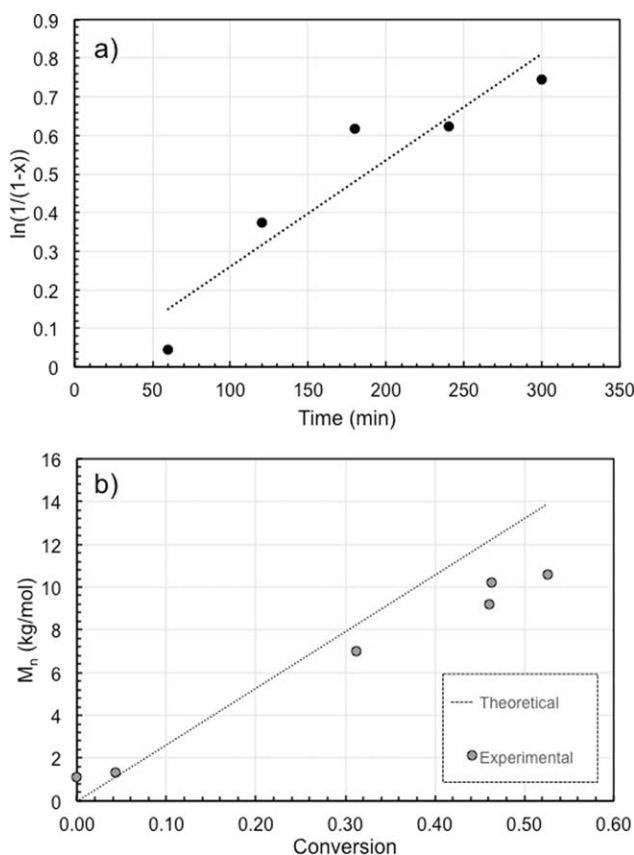


Figure 4. (a) Representative kinetic plot (scaled conversion of $\ln[(1-x)^{-1}]$ (x = conversion) versus time) and (b) number average molecular weight *M*_n versus conversion (bottom) for SAN copolymers with feed composition S:AN (in mol %) of 70:30.

Table VI. Formulation and Characterization of SAN Macroinitiator and SAN-*b*-S/*t*BA Block Copolymer by Nitroxide Mediated Polymerization

Experiment ID	Feed composition			Characterization				
	[NHS-BB] (M) ^a	[S] ₀ (M) ^a	[AN] ₀ (M) ^a	<i>f</i> _{S,0}	<i>F</i> _S ^b	<i>M</i> _n (kg mol ⁻¹) ^c	<i>D</i> ^c	
S/AN_60/40	0.019	3.43	2.42	0.60	0.62	10.0	1.23	
Experiment ID	[S/AN 60/40] (M) ^d	[S] ₀ (M) ^d	[<i>t</i> BA] ₀ (M) ^d	<i>f</i> _{S,0}	<i>F</i> _S ^b	<i>F</i> _{AN} ^b	<i>M</i> _n (kg mol ⁻¹) ^c	<i>D</i> ^c
S/AN- <i>b</i> -S/ <i>t</i> BA	0.002	2.02	2.02	0.50	0.74	0.16	36.6	1.34

^a 50:50 wt % ratio of monomers to solvent.

^b Calculated using ¹H-NMR.

^c Measured with respect to PMMA standards at 40 °C using THF as the mobile phase.

^d 50:50 wt % ratio of monomers to solvent and the macroinitiator is S/AN_60/40.

of dead chains in the SAN macroinitiator. The *t*-BA groups were cleaved with trifluoroacetic acid to yield carboxylic acid groups, which gave the block copolymer the necessary acid functionality for reactive extrusion. The first block had a composition (S:AN) of 62:38 mol %. With the second block, the overall copolymer had an AA composition of 10 mol % (~40 AA groups per chain) and an overall AN composition of about 16 mol %. It seems that the AN loading is low to be an effective barrier material, but recall that the AN is contained within a single block and if desired can be manipulated by the feed content for the first block and the chain length of the second block.

Extrusion and SEM Analysis

Prior to extrusion, the SG1 group of the S_AN_NHS_BB copolymers and SAN-*b*-SAA used in extrusion was cleaved to increase the thermal stability.³² S_AN_NHS_BB-4, S/AN/AA_8, and S/AN-*b*-S/AA were each extruded with PE-*g*-GMA at 160 °C. Blend miscibility was estimated theoretically by evaluating the enthalpic interaction parameter (χ_{blend}), which can be calculated by eq. (2):

$$\chi_{\text{blend}} = \chi_{A/B} = \frac{v}{RT} \times (\delta_A - \delta_B)^2 \quad (2)$$

where, χ_{blend} is the interaction parameter between PE-*g*-GMA (A) and the polymer (B), *R* is the gas constant, *T* is absolute temperature of the blend, *v* is the molar volume, and δ is the Hildebrand solubility parameter. χ_{blend} for each blend was estimated. The δ for PE-*g*-GMA was about 7.90 cal^{1/2} cm^{-3/2} while

the δ for non-functional SAN (S_AN_NHS_BB-4) was estimated as 9.9 cal^{1/2} cm^{-3/2} and the δ for functional SANs were 9.6 cal^{1/2} cm^{-3/2} and 9.7 cal^{1/2} cm^{-3/2}. χ_{blend} for all three blends is quite high, ranging from 0.34 to 0.47, suggesting that the blends were immiscible.⁷⁵ The molar volumes were calculated from the geometric mean molar volume of the individual components from their density and monomer molecular weights. Furthermore, δ of the SAN copolymer was determined by using a weighted average (using the polymer compositions as the weights) of the solubility parameters found in the literature for the homopolymers.⁷⁵

The *in situ* reaction between the complementary functional groups will result in the formation of a graft copolymer at the interface, which will reduce the coalescence significantly.³² The non-reactive blend does not possess complementary functional groups so the blend should show signs of significant coalescence. Therefore, SEM images post-extrusion and post-annealing were used to verify the effect of compatibilization. It should be noted that there is not a common solvent between SAN and PE, and thus any confirmation of chain coupling via GPC cannot be determined. The SEM images are shown in Figure 6 for blends involving PE-*g*-GMA/S_AN_NHS_BB-4 (non-reactive) and PE-*g*-GMA/(S/AN-*b*-S/AA) (reactive blend with SAN copolymer made by NMP) and Figure 7 for the blend involving PE-*g*-GMA/(S/AN/AA) (reactive blend with terpolymer made by conventional radical polymerization). The quantitative analysis in terms of particle size is shown in Tables VII and VIII.

$\langle D \rangle_{\text{vs}}$ estimates the ratio of volume to interfacial area. $\langle D \rangle_{\text{vs}}$ is used as it relates to the interfacial coverage of the compatibilizing copolymer around the dispersed phase particle.⁷⁶ For example, $\langle D \rangle_{\text{vs}}$ can be used to estimate how much graft copolymer is formed at the interface. Particle size analysis showed that the reactive blends yielded similar $\langle D \rangle_{\text{vs}} = 1.7 \mu\text{m}$ (SAN-*b*-SAA) and 1.1 μm (S/AN/AA), respectively, while the non-reactive blend had a $\langle D \rangle_{\text{vs}} = 3.0 \mu\text{m}$. It was expected that the acid-epoxy reaction would generate enough copolymer at the interface to see a more drastic difference in the domain sizes. Without coalescence prevention, and given the relatively slow kinetics (<10% conversion within the first 2 min at 180 °C) of the acid-epoxy reaction,⁴⁹ little reaction during extrusion was likely. However, annealing showed that the reactive blends were sufficiently stable whereas the non-reactive blend dramatically coarsened (domain size increased by a factor of 4). Longer extrusion times or addition of a catalyst might have helped to reduce the

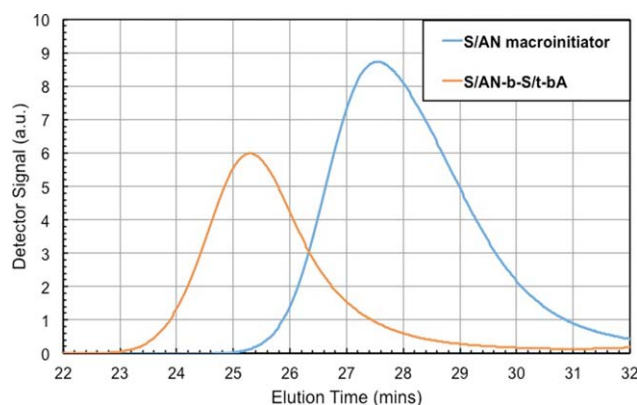


Figure 5. GPC chromatograph for chain extension of SAN macro-initiator with a batch of styrene/*t*-butyl acrylate (S/*t*-BA). [Color figure can be viewed in the online issue, which is available at wileyonlinelibrary.com.]

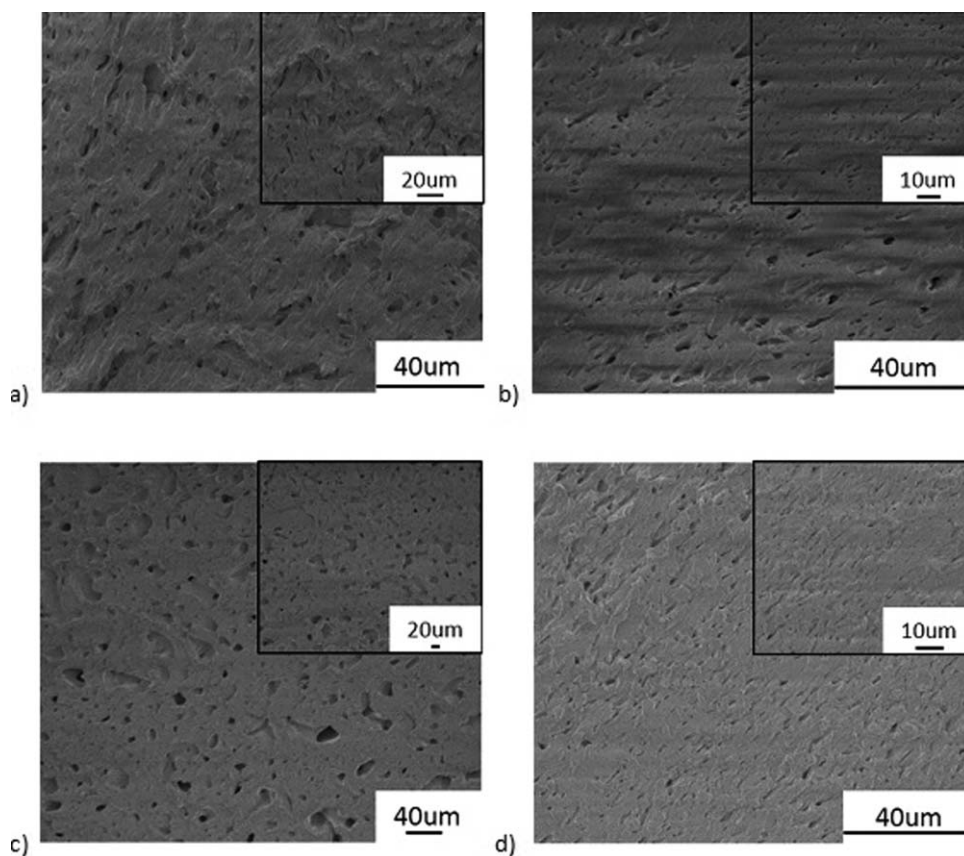


Figure 6. SEM images of (a) 70 wt % PE-g-GMA, 30 wt % SAN after extrusion and freeze fracturing, (b) 70 wt % PE-g-GMA, 30 wt % SAN-b-S/AA after extrusion and freeze fracturing, (c) 70 wt % PE-g-GMA, 30 wt % SAN post annealing, (d) 70 wt % PE-g-GMA, 30 wt % SAN-b-S/AA post annealing.

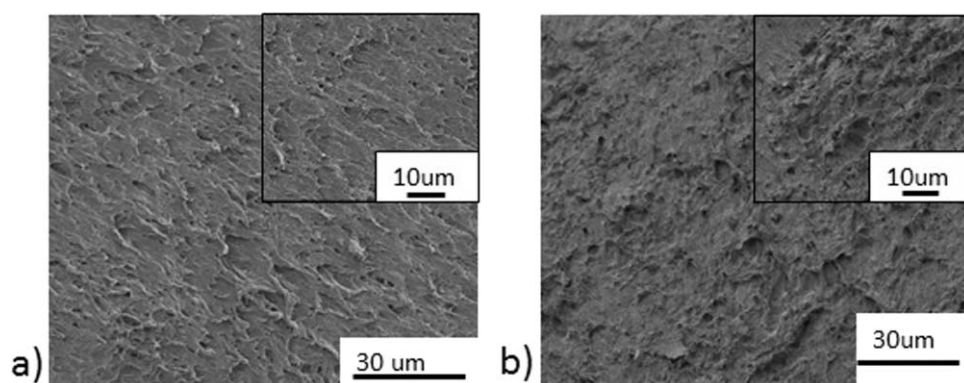


Figure 7. SEM images of (a) 70 wt % PE-g-GMA, 30 wt % S/AN/AA_8 after extrusion and freeze fracturing, 70 wt % PE-g-GMA, 30 wt % S/AN/AA_8 post annealing.

Table VII. Particle Analysis of SEM Images for PE-g-GMA Blends with Non-functional SAN and Acid-functional SAN-*b*-(S/AA) Block Copolymer

SEM image	Blend ratio			Annealing conditions	$\langle D \rangle_{vs}$ (μm)
	PE-g-GMA (wt %)	SAN- <i>b</i> -S/AA (wt %)	SAN_NHS_BB-4 (wt %)		
Figure 5(a)	70	0	30	None	3.0
Figure 5(b)	70	30	0	None	1.7
Figure 5(c)	70	0	30	18 h at 150°C	12.6
Figure 5(d)	70	30	0	18 h at 150°C	1.6

Table VIII. Particle Analysis of SEM Images for PE-g-GMA blends with S/AN/AA Terpolymer

sem image	Blend ratio		Annealing conditions	$\langle D \rangle_{vs}$ (μm)
	PE-g-GMA (wt %)	S/AN/AA_8 (wt %)		
Figure 6(a)	70	30	None	1.1
Figure 6(b)	70	30	18 hrs at 150 °C	2.1

reactive blend particle more. A previous study was able to achieve a 30% conversion with this reaction coupling with a residence time of 10 min.⁷⁷ To increase the coupling rate, a catalyst was used to push the conversion to 80%.⁷⁷

Besides the immiscibility, the interfacial tension of the blends was estimated using eq. (3).⁷⁸

$$\Gamma = \left(\frac{\chi}{6}\right)^{1/2} \times p_o b k T \quad (3)$$

Here, χ is the interaction parameter, k is the Boltzmann constant, T is the temperature, b is the statistical segment length, and p_o is the average monomer density. The monomer density and the statistical segment length were estimated using a weighted average with the weights as the polymer compositions and blend ratios. The statistical segment lengths b were calculated using tabulated data⁷⁹ and are given as follows [=] nm (g mol)^{-1/2}: $b_{\text{poly}(\text{acrylonitrile})} = 0.093$, $b_{\text{poly}(\text{styrene})} = 0.068$, $b_{\text{poly}(\text{acrylic acid})} = 0.067$, $b_{\text{poly}(\text{ethylene})} = 0.10$. The interfacial tension for the functionalized blends was estimated to be 13 mN m⁻¹ (SAN-*b*-SAA) and 14 mN m⁻¹ (S/AN/AA), and 15 mN m⁻¹ for the non-functional blend. Previous studies have shown that the interfacial tension for blends containing polyethylene, copolymers of styrene and acrylonitrile or polymers structurally similar to these varies significantly depending on composition, blend ratio, and temperature.^{80–87} These reported values are lower than those approximated by eq. (3). It should be noted that eq. (3) is a simple model that assumes symmetric properties for both polymers along with incompressibility and an infinite degree of polymerization.⁷⁸

The interfacial tensions can be used in conjunction with eq. (4), Taylor's equation, to compare the theoretical particle size with the observed domains.⁵³

$$\langle D \rangle_{vs} = \frac{4\Gamma(\eta_r + 1)}{\dot{\gamma}\eta_m\left(\frac{19}{4}\eta_r + 4\right)} \quad (4)$$

Here, Γ is the interfacial tension, η_r is the viscosity ratio between the dispersed phase and the matrix, $\dot{\gamma}$ is the shear rate, and η_m is the viscosity of the matrix. The estimated particle size by eq. (4) at a maximum shear rate of 27 s⁻¹ for the functionalized blend (SAN-*b*-SAA) and non-functional blend was 0.28 μm and 0.33 μm , respectively. The shear rate was found using the rotational speed (50 rpm), along with the known gap distance of about 1.40 mm by eq. (5):

$$\dot{\gamma}_{\text{max}} = \frac{\pi \times D \times N}{\text{gap distance}} \quad (5)$$

where D is the diameter of the screw and N is the rotational speed of the screw.

These estimates for the reactive and non-reactive blend dispersed phase particle sizes are lower than the observed particle sizes as Taylor's equation does not take into account coalescence in the blend. Therefore, the observed particle sizes were compared to Wu's equation [eq. (6)], a semi-empirical model, which accounts for coalescence intrinsically.⁵³

$$\langle D \rangle_{vs} = \frac{4\Gamma\eta_r^{-0.84}}{\dot{\gamma}\eta_m} \quad (6)$$

The estimated particle size by eq. (6) at the maximum shear rate of 27 s⁻¹ for the functionalized (SAN-*b*-SAA) and non-functionalized blends were 20 μm and 25 μm , respectively, which are higher than the observed data due to the very low viscosity ratio. Note that Wu's equation is limiting—it is for shear rates ~ 100 s⁻¹ and dispersed phase concentrations of 15 wt %. Note that increasing the shear rate to 100 s⁻¹ would have resulted in calculated particle sizes similar to the non-reactive blend. Further note that the η_m and η_r used in the predicted equations were obtained from the rheological data described in the following section.

Rheology

The complex viscosity of the non-reactive SAN copolymer (S_AN_NHS_BB-4), SAN-*b*-SAA, and PE-g-GMA was measured at 160 °C and is shown below in Figure 8.

For the particular extruder used, the shear rate was approximated using the largest and smallest diameter of the screws at a rotational speed of 50 rpm. The shear rates were approximated as 27 and 9 s⁻¹. In this interval, the viscosity ratio (η_p) of the polymer to PE-g-GMA is approximately 0.03. For the best dispersion, $\eta_p \approx 1$ should result in the smallest domain sizes.^{32,73,88–90} Obviously, mixing could have improved with a higher η_p and this is due to the relatively low molecular weight SAN-*b*-S/AA copolymer used. Our previous study with SAN/PE blends (using an amine/anhydride reaction where the SAN was terminated with a single amine group and the PE was grafted with maleic anhydride (MA)) had similar $\eta_p \sim 0.04$ at shear rates ~ 10 – 100 s⁻¹ and the SAN particle size was stable and $\langle D \rangle_{vs} \sim 2$ μm .¹⁰ In another study, using the same extruder, we blended a methyl acrylate (MA)/AN/4-*para*-aminostyrene

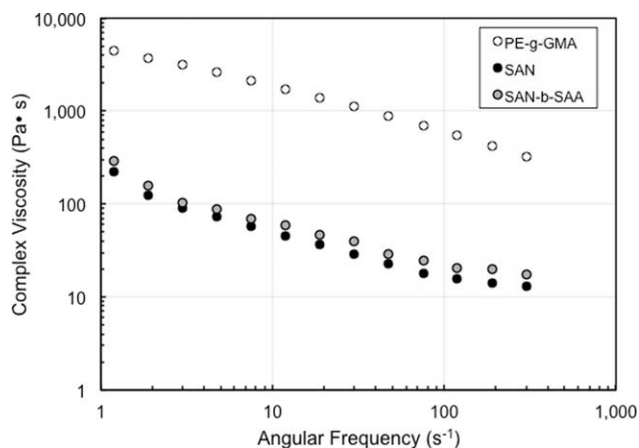


Figure 8. Complex viscosity at 160 °C versus angular frequency measurements for PE-g-GMA (blue), non-reactive SAN (orange, sample S_AN_NHS_BB-4), and SAN-*b*-SAA (gray).

(PAS) terpolymer made by conventional radical polymerization containing several pendant amine groups into PE-g-MA, and we obtained sub-micron particle sizes. In this case, $\eta_r \sim 0.5$ at the shear rates of interest. There are obviously several factors at play in compatibilization/mixing of polymer blends: interfacial tension (and hence interfacial thickness which can limit the amount of copolymer formed), type of reaction and the rheology of the individual components. Here, we showed that the epoxy/acid reaction (which is easy to incorporate with the respective homopolymers) is effective at producing stable morphologies of SAN/PE blends with relatively small particle sizes. These results will serve as impetus for further work toward orienting SAN domains in the PE for more effective barrier morphologies and eventually for permeation testing.

CONCLUSIONS

In this study, AN-containing polymers with and without an acid functionality were synthesized by NMP. They were each melt blended with PE-GMA, a poly(ethylene) grafted with epoxy-functional glycidyl methacrylate, at 160°C at 50 rpm. The domain size of the SAN dispersed phase was 1.1 μm , 1.7 μm , and 3.0 μm when functional (via AA terpolymerization by conventional radical polymerization, and as a block copolymer synthesized by NMP), and non-functional SAN was used, respectively. Upon annealing, evidence of significant coalescence was seen for the non-reactive blend as its domain size increased to 12.6 μm . The domain size for the reactive blend did not coarsen significantly, indicating that sufficient acid-epoxy coupling reaction occurred to maintain a stable morphology. When the reactive terpolymer was used as the dispersed phase, it yielded a smaller domain size in PE-g-GMA than the block copolymer after initial mixing, but increased slightly after annealing, perhaps due to the greater compositional heterogeneity induced by using conventional radical polymerization.

ACKNOWLEDGMENTS

Authors thank Imperial Oil (University Research Award) and NSERC CRD (Grant # 412508-2011) and McGill University (EUL scholarship for AG) for their generous funding. Authors would like to express their deepest thanks to Frederick Morin (NMR), Peter Fiurasek (TGA, DSC, ATR), David Liu (SEM), and Hanno Erythropel (rheology) for their training and guidance regarding the use of the various instruments.

REFERENCES

1. Allen, S. M.; Fujii, M.; Stannett, V.; Hopfenberg, H. B.; Williams, J. L. *J. Membr. Sci.* **1977**, *2*, 153.
2. El-Sabee, M. Z.; Ahmed, A. H.; Mawaziny, S. *Eur. Polym. J.* **1974**, *10*, 1149.
3. Dunn, P.; Ennis, B. C. *J. Appl. Polym. Sci.* **1970**, *14*, 1795.
4. Frushour, B. *Polym. Bull.* **1984**, *11*, 375.
5. Krigbaum, W. R.; Tokita, N. *J. Polym. Sci.* **1960**, *43*, 467.
6. Rangarajan, P.; Yang, Y.; Godshall, D.; McGrath, J.; Wilkes, G.; Baird, D. *J. Appl. Polym. Sci.* **2002**, *85*, 69.
7. Bhanu, V. A.; Rangarajan, P.; Wiles, K.; Bortner, M.; Sankarpandian, M.; Godshall, D.; Glass, T. E.; Banthia, A. K.; Yang, J.; Wilkes, G.; Baird, D.; McGrath, J. E. *Polymer* **2002**, *43*, 4841.
8. Iwakura, Y.; Tamikado, T.; Yamaguchi, M.; Takei, K. *J. Polym. Sci.* **1959**, *39*, 203.
9. Lewis, F. M.; Mayo, F. R.; Hulse, W. F. *J. Am. Chem. Soc.* **1945**, *67*, 1701.
10. Nicolas, J.; Brusseau, S.; Charleux, B. *J. Polym. Sci. Part A: Polym. Chem.* **2010**, *48*, 34.
11. Pichot, C.; Zaganianis, E.; Guyot, A. *J. Polym. Sci. Polym. Symp.* **1975**, *52*, 55.
12. Zengeni, E.; Hartmann, P. C.; Sanderson, R. D.; Mallon, P. E. *J. Appl. Polym. Sci.* **2011**, *119*, 1060.
13. Améduri, B.; Boutevin, B.; Gramain, P. *Adv. Polym. Sci.* **1997**, *127*, 87.
14. Baumann, M.; Roland, A.; Schmidt-Naake, G.; Fischer, H. *Macro Mater. Eng.* **2000**, *280*, 1.
15. Ceresa, R. J. *Polymer* **1960**, *1*, 488.
16. Climie, I. E.; White, E. F. T. *J. Polym. Sci.* **1960**, *47*, 149.
17. Fan, D.; He, J.; Xu, J.; Tang, W.; Liu, Y.; Yang, Y. *J. Polym. Sci. Part A: Polym. Chem.* **2006**, *44*, 2260.
18. Fukuda, T.; Terauchi, T.; Goto, A.; Tsujii, Y.; Miyamoto, T. *Macromolecules* **1996**, *29*, 3050.
19. Mahato, B.; Maiti, S. *Colloid Polym. Sci.* **1988**, *266*, 601.
20. Mazzucco, M. L.; Marchesin, M. S.; Fernades, E. G.; Da Costa, R. A.; Marini, R.; Bretas, R. J.; Bartoli, J. *J. Compos. Mater.* **2016**, *50*, 771.
21. Penfold, H. V.; Holder, S. J.; McKenzie, B. E. *Polymer* **2010**, *51*, 1904.
22. Tang, C. T.; Kowalewski, T.; Matyjaszewski, K. *Macromolecules* **2003**, *36*, 8587.
23. Tsarevsky, N. V.; Sarbu, T.; Gobelt, B.; Matyjaszewski, K. *Macromolecules* **2002**, *35*, 6142.
24. Gromadzki, D.; Lokaj, J.; Černoč, P.; Diat, O.; Nallet, F.; Štěpánek, P. *Eur. Polym. J.* **2008**, *44*, 189.
25. Gromadzki, D.; Lokaj, J.; Šlouf, M.; Štěpánek, P. *Polymer* **2009**, *50*, 2451.
26. Dhoot, S. N.; Freeman, B. D.; Stewart, M. E. *Barrier Polymers in Encyclopedia of Polymer Science and Technology*, 4th ed.; Wiley: New York, NY, **2002**.
27. Fortelný, I.; Mikešová, J.; Hromádková, J.; Hašová, V.; Horák, Z. *J. Appl. Polym. Sci.* **2003**, *90*, 2303.
28. Leal, L. J. *Central South Univ. Technol.* **2007**, *14*, 1.
29. Lyu, S.; Bates, F. S.; Macosko, C. W. *AIChE J.* **2000**, *46*, 229.
30. Marić, M.; Ashurov, N.; Macosko, C. W. *Polym. Eng. Sci.* **2001**, *41*, 631.
31. Marić, M.; Macosko, C. W. *J. Polym. Sci. Part B: Polym. Phys.* **2002**, *40*, 346.
32. Oxby, K. J.; Marić, M. *Macromol. React. Eng.* **2014**, *8*, 160.
33. Zou, Z.; Sun, Z.; An, L. *Chin. J. Polym. Sci.* **2014**, *32*, 255.

34. Bell, J. R.; Chang, K.; López-Barrón, C. R.; Macosko, C. W.; Morse, D. *Macromolecules* **2010**, *43*, 5024.
35. Galloway, J.; Jeon, H. K.; Bell, J. E.; Macosko, C. W. *Polymer* **2005**, *46*, 183.
36. Kipp, D.; Ganesan, V. J. *Phys. Chem. B* **2014**, *118*, 4425.
37. Lee, C. W.; Kim, E. S.; Yoon, J. S. *J. Appl. Polym. Sci.* **2005**, *98*, 886.
38. Leibler, L. *Makromol. Chem. Macromol. Symp.* **1988**, *16*, 1.
39. Pospiech, D. In *Polymer Surfaces and Interfaces: Characterization, Modification and Applications*; editor Stamm, M. Springer: Berlin, **2008**; p 275.
40. Wacharawichanant, S.; Amorncharoen, P.; Wannasirichoke, R. *Polym. Plast. Technol. Eng.* **2015**, *54*, 1349.
41. Fina, A.; Monticelli, O.; Camino, G. *J. Mater. Chem* **2010**, *20*, 9297.
42. Oyama, H. T. *Polymer* **2009**, *50*, 747.
43. Pagnoulle, C.; Jérôme, R. *Macromolecules* **2001**, *34*, 965.
44. Pernot, H.; Baumert, M.; Court, F.; Liebler, L. *Nat. Mater.* **2002**, *1*, 54.
45. Spinella, S.; Cai, J.; Samuel, C.; Zhu, J.; McCallum, S. A.; Habibi, Y.; Raquez, J. M.; Dubois, P.; Gross, R. A. *Biomacromolecules* **2015**, *16*, 1818.
46. Tao, Y.; Lebovitz, A. H.; Torkelson, J. M. *Polymer* **2005**, *46*, 4753.
47. Yang, H.; Ma, J.; Li, W.; Liang, B.; Yu, Y. *Polym. Eng. Sci.* **2002**, *42*, 1629.
48. Moon, B.; Hoyer, T. R.; Macosko, C. W. *Macromolecules* **2001**, *34*, 7941.
49. Orr, C.; Cernohous, J. J.; Guegan, P.; Hirao, A.; Jeon, H. K.; Macosko, C. W. *Polymer* **2001**, *42*, 8171.
50. Turunen, M. P. K.; Laurila, T.; Kivilahti, J. K. *J. Appl. Polym. Sci.* **2006**, *101*, 3689.
51. Liu, N. C.; Baker, W. E. *Adv. Polym. Technol.* **1992**, *11*, 249.
52. Xanthos, M.; Dagli, S. S. *Polym. Eng. Sci.* **1991**, *31*, 929.
53. Marić, M.; Macosko, C. W. *Polym. Eng. Sci.* **2001**, *41*, 118.
54. Jeon, H. K.; Macosko, C. W.; Moon, B.; Hoyer, B.; Yin, T. R. *Z. Macromolecules* **2004**, *37*, 2563.
55. Vinas, J.; Chagneux, N.; Gimes, D.; Trimaille, T.; Favier, A.; Bertin, D. *Polymer* **2008**, *49*, 3639.
56. Li, X.; Wang, L.; Koseki, H. *J. Hazard. Mater.* **2008**, *159*, 13.
57. Lessard, B.; Schmidt, S. C.; Marić, M. *Macromolecules* **2008**, *41*, 3446.
58. Smith, B. *Fundamentals of Fourier Transform Infrared Spectroscopy*; CRC Press, Boca Raton FL, **1995**.
59. Hill, D. J. T.; Lang, A. P.; O'Donnell, J. H.; O'Sullivan, P. W. *Eur. Polym. J.* **1989**, *25*, 911.
60. Ritchey, W. M.; Ball, L. E. *J. Polym. Sci. Part Part B: Polym. Lett* **1966**, *4*, 557.
61. Sanghvi, P. G.; Patel, A. C.; Gopalkrishnan, K. S.; Devi, S. *Eur. Polym. J.* **2000**, *36*, 2275.
62. Otsu, T. *Makromol. Chem. Macromol. Symp.* **1987**, *10*, 235.
63. Florjańczyk, Z.; Lukasik, L.; Prokopowicz, L. *Polimery (Poland)* **1991**, *36*, 177.
64. Massey, L. K. *Permeability Properties of Plastics and Elastomers*; William Andrew, Norwich, NY, **2003**.
65. Beevers, R. B. *J. Polym. Sci. Part A: Polym. Chem.* **1964**, *2*, 5257.
66. Bonardelli, P.; Moggi, G.; Turturro, A. *Polymer* **1986**, *27*, 905.
67. Rieger, J. J. *Therm. Anal.* **1996**, *46*, 965.
68. McGaugh, M. C.; Kottle, S. J. *J. Polym. Sci. Part B: Polym. Phys.* **1967**, *5*, 817.
69. Pfäffli, P.; Zitting, A.; Vainio, H. *Scand. J. Work Environ. Health* **1978**, *4*, 22.
70. Marić, M.; Consolante, V. *J. Appl. Polym. Sci.* **2013**, *127*, 3645.
71. Lessard, B.; Marić, M. *Macromolecules* **2008**, *41*, 7881.
72. Matyjaszewski, K.; Spanswick, J. *Mater. Today* **2005**, *8*, 26.
73. Wu, S. *Polymer* **1987**, *28*, 1144.
74. Barton, A. *Handbook of Polymer-Liquid Interaction Parameters and Solubility Parameters*; CRC Press, Boca Raton, FL, **1990**.
75. Emerson, J. A.; Toolan, D. T. W.; Howse, J. R.; Furst, E. M.; Epps, T. H., III. *Macromolecules* **2013**, *46*, 6533.
76. Macosko, C. W.; Guégan, P.; Khandpur, A. K.; Nakayama, A.; Marechal, P. T.; Inoue, T. *Macromolecules* **1996**, *29*, 5590.
77. Taha, M.; Perrut, V.; Roche, A. A.; Pascault, J. P. *J. Appl. Polym. Sci.* **1997**, *65*, 2447.
78. Anastasiadis, S. H.; Chen, J. K.; Koberstein, J. T.; Sohn, K. E.; Emerson, J. A. *Polym. Eng. Sci.* **1986**, *26*, 1410.
79. Brandrup, J.; Immergut, E. H.; Grulke, E. A. *Polymer Handbook*, 4th ed.; Wiley, New York, NY, **2003**.
80. Wu, S. *J. Phys. Chem.* **1970**, *74*, 632.
81. Shariatpanahi, H.; Nazokdast, H.; Hemmati, M. *J. Appl. Polym. Sci.* **2003**, *88*, 54.
82. Jung, H. J.; Son, Y.; Park, O. O. *Macromol. Res.* **2014**, *22*, 146.
83. Gong, P.; Oshima, M. *J. Appl. Polym. Sci.* **2013**, *131*, 39228.
84. Mekhilef, N.; Carreau, P.; Favis, B.; Martin, P.; Ouhlal, A. *J. Polym. Sci. Part B: Polym. Phys.* **2000**, *38*, 1359.
85. Kim, J. H.; Kim, M. J.; Kim, C. K.; Lee, J. W. *Korea-Aust Rheol. J.* **2001**, *13*, 125.
86. Elemans, P. H. M.; Janssen, J. M. H.; Meijer, H. E. H. *J. Rheol.* **1990**, *34*, 1311.
87. Chappleau, N.; Favis, B. D.; Carreau, P. J. *J. Polym. Sci. Part B: Polym. Phys.* **1998**, *36*, 1947.
88. Favis, B. D.; Chalifoux, J. P. *Polym. Eng. Sci.* **1987**, *27*, 1591.
89. Grace, H. P. *Chem. Eng. Commun.* **1982**, *14*, 225.
90. Taylor, G. I. *Proc. Roy. Soc.* **1932**, *A135*, 685.